Ephrin-B2 promotes gastric cancer growth by inhibiting apoptosis and regulating the cell cycle via the Wnt/β-catenin signaling pathway

DING DING[1,2], XIAOSHAN WANG[1], RAN XUAN[2], RUI LI[2], YALU ZHANG[3] and ZHENGGUANG WANG[1]

[1]Department of General Surgery, The First Affiliated Hospital of Anhui Medical University, Hefei, Anhui 230022, P.R. China; [2]Department of General Surgery, The Third Affiliated Hospital of Anhui Medical University (The First People's Hospital of Hefei), Hefei, Anhui 230061, P.R. China; [3]Department of General Surgery, The First Affiliated Hospital of University of Science and Technology of China, Division of Life Science and Medicine, University of Science and Technology of China, Hefei, Anhui 230001, P.R. China

Received April 17, 2025; Accepted October 22, 2025

DOI: 10.3892/ijo.2025.5821

Abstract. Gastric cancer (GC) ranks among the most prevalent malignancies worldwide and is associated with high mortality rates. Ephrin-B2 (EFNB2), a membrane-bound ligand that interacts with Eph receptor tyrosine kinases, has been implicated in various cancer-related biological processes; however, its precise role in GC remains poorly understood. By integrating data from multiple public databases with immunohistochemical analyses of tissue microarrays, significant upregulation of EFNB2 expression in GC specimens compared with paired adjacent normal tissue was demonstrated. Elevated EFNB2 levels were associated with the poor overall survival and disease-free survival in patients with GC. EFNB2 knockdown inhibited cellular proliferation and viability, increased apoptosis, and induced cell cycle arrest at the G_0/G_1 phase in GC cells. By contrast, EFNB2 overexpression resulted in the opposite oncogenic effects. Mechanistically, rescue experiments identified the Wnt/β-catenin signaling cascade as the primary molecular pathway mediating EFNB2-driven tumorigenic effects. These results were further validated *in vivo* using cell-derived xenograft models, which confirmed the key role of Wnt/β-catenin pathway activation in EFNB2-induced tumor progression. Collectively, these results suggested that EFNB2 represents a promising molecular target for therapeutic intervention in GC.

Introduction

Gastric cancer (GC) is the fifth most common malignancy and the fifth leading cause of cancer-related mortality worldwide (1). Several factors contribute to GC initiation and progression, including *Helicobacter pylori* (HP) infection, chronic gastritis and genetic alterations (2,3). Despite its high incidence, GC is often diagnosed at an advanced stage due to the non-specific nature of its clinical symptoms. Consequently, late detection typically leads to poor prognosis, with the 5-year survival rate remaining <30% (4,5). This scenario underscores the urgent need to identify novel therapeutic targets to enhance treatment efficacy for GC.

The Eph receptor family, first identified in a human hepatocellular carcinoma cell line known for erythropoietin production, has been implicated in multiple types of cancer due to its frequent upregulation in receptor tyrosine kinase (RTK) screenings (6). For example, ephrin-A1 is upregulated in hepatocellular carcinoma and drives its progression by promoting proliferation and invasion (7). Ephrin-B3 expression is upregulated in glioma biopsies and promotes invasion of glioma cells (8). This discovery emerged during research aimed at identifying novel tyrosine kinase receptors, highlighting the significance of Eph receptors in oncogenic processes (9). Ephrin-B2 (EFNB2), a membrane-anchored ligand of the Eph family of RTKs (10), interacts with the EphB4 receptor as part of the largest RTK subfamily. The EFNB2-EphB4 signaling axis serves a key role in regulating cellular adhesion and repulsion in diverse biological contexts (11,12). Furthermore, EFNB2 can function in a cell-autonomous manner, independent of Eph receptor interactions, and participates in complex signaling pathways, including the AKT/mTOR and ERK pathways (13-15), thereby modulating various physiological events. Notably, EFNB2 has been demonstrated to regulate malignant progression in various tumor cells (15-18). For instance, EFNB2 is highly expressed in pancreatic cancer, and facilitates proliferation, migration and invasion of pancreatic cancer via activation of the p53/p21 signaling axis (16). Conversely, EFNB2 expression has been associated with good prognosis in breast cancer, and is known to inhibit cell proliferation and migration (17). However, to the best of our knowledge, the role of EFNB2 in GC remains unclear and requires further investigation.

Correspondence to: Professor Zhengguang Wang, Department of General Surgery, The First Affiliated Hospital of Anhui Medical University, 218 Jixi Road, Shushan, Hefei, Anhui 230022, P.R. China
E-mail: wangzhengguang@ahmu.edu.cn

Key words: gastric cancer, ephrin-B2, proliferation, apoptosis, cell cycle, Wnt/β-catenin signaling pathway

Integrated genomic analysis has identified dysregulation of the Wnt/β-catenin pathway in ~46% of GC cases (19). This evolutionarily conserved signaling pathway, frequently disrupted by component mutations, regulates key cellular processes, including fate determination, proliferation, differentiation, migration, apoptosis and stemness maintenance (20-22). Under basal conditions, β-catenin levels are tightly controlled by a destruction complex containing GSK3β, which targets β-catenin for proteasomal degradation through ubiquitination-dependent mechanisms (21). Upon pathway activation, stabilized β-catenin is translocated into the nucleus, where it forms transcriptional complexes with co-activators to modulate gene expression programs, including c-myc controlling cell proliferation and differentiation (21,22). Considering the potential roles of EFNB2 and the Wnt/β-catenin pathway in tumors, we hypothesized that EFNB2 may regulate the malignant progression of GC through the Wnt/β-catenin signaling cascade.

The present study investigated the expression levels of EFNB2 and its prognostic significance in patients with GC through a comprehensive analysis of public databases and tissue microarray (TMA)-based immunohistochemical (IHC) assessment. To further elucidate the functional roles of EFNB2 in GC pathogenesis, a series of cellular assays were carried out and murine models were established to examine its regulatory effects on cellular proliferation, apoptotic processes and cell cycle progression both *in vitro* and *in vivo*. Mechanistically, CHIR99021 and differentiation-inducing factor-3 (DIF-3) were employed to assess whether the effects of EFNB2 were primarily mediated through the Wnt/β-catenin signaling cascade.

Materials and methods

Bioinformatics analysis. Various public online databases, including Gene Expression Profiling Interactive Analysis (GEPIA) (23), LinkedOmics (24), Kaplan-Meier Plotter (25), Tumor Immune Estimation Resource (TIMER) (26) and Gene Expression Omnibus (GEO; https://www.ncbi.nlm.nih.gov/gds), were used to explore EFNB2 expression and prognosis, and perform associated analyses. In GEPIA, the option 'Match TCGA normal and GTEx data' was selected for EFNB2 expression analysis; the cutoff setting 'Cutoff-High versus Cutoff-Low: 30 versus 30' was employed for survival analysis; and Spearman correlation analysis was performed to assess the associations of EFNB2 with GSK3β, catenin β1 and MYC. In Kaplan-Meier Plotter, the option 'Exclude GSE62254' was selected for survival analysis (27). Therefore, the analysis included datasets GSE14210, GSE15459, GSE22377, GSE29272 and GSE51105 (28-32), with the cutoff set to 'Auto select best cutoff'. Other parameters were left at the default. Additionally, two GEO datasets (GSE13195 and GSE184336) were used to compare the expression levels of EFNB2 and perform correlation analyses (33,34).

Tissue samples. A commercial GC tissue microarray (cat. no. HStmA180Su3) was purchased from Shanghai Outdo Biotech Co., Ltd., consisting of 96 GC tissues and 84 adjacent normal tissues (ANTs) collected between December 2013 and September 2015. The mean age of the patients was 59 years, with a range of 40-83 years. The inclusion criteria were as follows: i) Age ≥18 years, ii) pathologically diagnosed with gastric adenocarcinoma; and iii) underwent radical gastrectomy. The exclusion criteria included the following: i) Underwent preoperative radiotherapy or chemotherapy; ii) pathological specimens unavailable; iii) mortality within 1 month following operation; and iv) refusal to participate in follow-up. Levels of the tumor markers AFP, CEA, CA50, CA125, CA153 and CA199 were assessed in patients with GC 1-3 days prior to surgery. Comprehensive clinical, pathological and follow-up data were available for all participants, with the exception of 24 patients lacking HP infection data and 2 patients with missing HER2 expression data. The diagnosis and staging were examined based on the 8th edition of the American Joint Committee on Cancer guidelines (35). Patients underwent follow-up every 3-6 months, with a maximum follow-up of 60 months. Among the 96 cases, 67 patients died between June 2014 and March 2020, while the remaining 29 patients survived until the end of the follow-up period. The clinicopathological characteristics of the patients with GC are presented in Table I. Ethical approval for the present study was obtained from the Ethics Committee of the First Affiliated Hospital of Anhui Medical University (approval no. 2024137; Hefei, China).

H&E, IHC and TUNEL staining. H&E and IHC staining of human and mouse GC tissues was conducted according to the standard procedures previously described (36,37). The sections were incubated with primary antibodies at 4˚C overnight. The antibodies used were as follows: EFNB2 antibody (1:500; cat. no. sc-398735; Santa Cruz Biotechnology, Inc.), β-catenin antibody (1:500; cat. no. 51067-2-AP; Proteintech Group, Inc.) and Ki67 antibody (1:500; cat. no. ab15580; Abcam). The One Step TUNEL Apoptosis Assay Kit (cat. no. C1088; Beyotime Biotechnology) was used according to the manufacturer's instructions. Briefly, tumor sections were fixed in 4% paraformaldehyde at 25˚C for 60 min and then washed three times with PBS. The TUNEL reaction solution was prepared by mixing 5 μl TdT enzyme with 45 μl fluorescent labeling solution. Each section was treated with 50 μl of the TUNEL solution at 37˚C for 60 min in the dark, and then washed three times with PBS. Finally, the sections were mounted with one drop of Antifade Mounting Medium with DAPI (1:1,000; cat. no. P0131; Beyotime Biotechnology) at 37˚C for 3 min and examined under an inverted fluorescence microscope (Olympus Corporation). Three random fields were captured for analysis. The percentage of Ki67 or TUNEL-positive cells was calculated as the number of positive cells/total number of cells per field.

TMA construction and IHC evaluation. A TMA of GC tissues and ANTs was constructed using formalin-fixed and paraffin-embedded blocks (cat. no. HStmA180Su32; Shanghai Outdo Biotech Co., Ltd.) to evaluate the expression levels of EFNB2. After IHC staining as described previously (36,37), TMA sections were scanned and digitalized using the Panoramic MIDI system (3D Histech; 3DHISTECH, Ltd.). IHC staining findings were independently assessed by two senior pathologists who were blinded to the clinical outcomes of the patients with GC. EFNB2 or β-catenin expression was quantified using an integrated IHC score, which combined

Table I. Relationship between EFNB2 expression and clinicopathological characteristics of patients with gastric cancer (n=96).

Parameters	Total, n	EFNB2 expression		P-value
		Low, n (n=48)	High, n (n=48)	
Age (years)				0.307
<60	47	26	21	
≥60	49	22	27	
Sex				0.811
Female	23	12	11	
Male	73	36	37	
Helicobacter pylori infection status				0.479
Negative	36	16	20	
Positive	36	19	17	
Missing value	24			
Tumor location				0.128
Cardia	15	4	11	
Gastric body	15	9	6	
Antrum	66	35	31	
Histological grade				0.128
G1	10	8	2	
G2	38	17	21	
G3	48	23	25	
Tumor size (cm)				<0.001[a]
<4	48	35	13	
≥4	48	13	35	
T stage				0.011[a]
T1-T2	25	18	7	
T3-T4	71	30	41	
Lymph node metastasis				0.369
Negative	28	16	12	
Positive	68	32	36	
M stage				0.037[a]
M0	83	45	38	
M1	13	3	10	
TNM stage				0.004[a]
I-II	46	30	16	
III-IV	50	18	32	
HER2				0.130[b]
Negative	87	45	42	
Positive	7	1	6	
Missing value	2			

[a]P<0.05; [b]The χ^2 test with Yates' continuity correction was used because two cells had an expected frequency <5 (minimum, 3.43). EFNB2, ephrin-B2.

both staining intensity and proportion (38,39). The samples were categorized into two groups according to the median IHC score: The low and high EFNB2 expression groups.

Cell culture and reagents. GC cell lines (MKN-45, AGS, MGC-803, BGC-823, and HGC-27) and the normal gastric mucosa epithelial cell line (GES-1) were obtained from The Cell Bank of Type Culture Collection of The Chinese Academy of Sciences. lAGS cells were cultured in F12 medium (HyClone; Cytiva). HGC-27 cells were cultured in DMEM (HyClone; Cytiva). MKN-45, MGC-803, BGC-823 and GES-1 cells were cultured in RPMI-1640 medium (HyClone; Cytiva). All media were supplemented with 10% FBS (Gibco; Thermo Fisher Scientific, Inc.) and 1% penicillin-streptomycin

(MilliporeSigma). The cells were cultured in a humidified incubator at 37˚C with 5% CO_2. For the rescue experiments, cells in designated groups were treated at 37˚C for 24 h with either CHIR99021 (5 μM; MedChemExpress) to activate the Wnt/β-catenin signaling cascade or DIF-3 (30 μM; MedChemExpress) to inhibit the Wnt/β-catenin signaling cascade.

Short hairpin RNA (shRNA/sh) and plasmid transfection. Transfection of GC cells was conducted using Lipofectamine® 2000 reagent (Invitrogen; Thermo Fisher Scientific, Inc.) according to the manufacturer's instructions. The shRNAs, the negative control (NC) shRNA, overexpression plasmids and empty vector were synthesized by Shanghai GeneChem Co., Ltd. hU6-MCS-CBh-gcGFP-IRES-puromycin was used as the vector for sh-EFNB2 and NC. The target sequence of EFNB2 shRNAs for AGS cells was as follows: sh1-EFNB2, 5'-CGATTTCCAAATCGATAGTTT-3'; and sh2-EFNB2, 5'-AGCAGACAGATGCACTATTAA-3'. A random sequence control shRNA (5'-TTCTCCGAACGTGTCACGT-3') was used as NC. For EFNB2 overexpression, HGC-27 cells were transfected with the pcDNA3.1-EGFP-P2A-EFNB2-3FLAG plasmid utilizing Lipofectamine® 2000 (Invitrogen; Thermo Fisher Scientific, Inc.). Empty vector was used as a control for overexpression experiments. The transfection protocol involved the introduction of 10 μg of the designated plasmids into the AGS or HGC-27 cells. GC cells were infected with the lentiviral vector at 37˚C for 48 h (MOI, 10). Following a 2-week selection with 4 μg/ml puromycin (Wuhan Servicebio Technology Co., Ltd.), the stable clones were kept in culture with a maintenance dose of 2 μg/ml of puromycin (Wuhan Servicebio Technology Co., Ltd.). After the 48-h transfection and subsequent 2-week selection, the efficiency of EFNB2 knockdown or overexpression was verified at the protein level.

Western blotting. Western blotting was conducted as previously described (25-27). GES-1, MKN-45, AGS, MGC-803, BGC-823 and HGC-27 cells were lysed with RIPA lysis buffer (Beyotime Biotechnology). This buffer is formulated to prevent protein degradation and preserve protein phosphorylation. The details of the primary antibodies used were as follows: EFNB2 (1:1,000; cat. no. sc-398735; Santa Cruz Biotechnology, Inc.), Bcl-2 (1:2,000; cat. no. ab182858; Abcam), Bax (1:2,000; cat. no. ab32503; Abcam), CyclinD1 (1:1,000, cat. no. 2978; Cell Signaling Technology, Inc.), CDK4 (1:1,000; cat. no. 12790; Cell Signaling Technology, Inc.), GSK3β (1:5,000; cat. no. 82061-1-RR; Proteintech Group, Inc.), phosphorylated (p-)GSK3β (Ser389; 1:1,000; cat. no. 14850-1-AP; Proteintech Group, Inc.), β-catenin (1:5,000; cat. no. 51067-2-AP; Proteintech Group, Inc.), c-myc (1:5,000; cat. no. 808451-RR; Proteintech Group, Inc.) and β-actin (1:1,000; cat. no. 4970; Cell Signaling Technology, Inc.). After incubation with the primary antibody at 4˚C overnight, the membranes were incubated with an HRP-labeled secondary antibody (1:5,000; cat. nos. ZB-5301 and ZB-5305; Beijing Zhongshan Jinqiao Biotechnology Co., Ltd.) and visualized using a Tanon 5200 Multi-Imaging System (Tanon Science and Technology Co., Ltd.).

Cell Counting Kit-8 (CCK-8) and colony formation assays. The protocols for the CCK-8 and colony formation assays have been described in detail previously (16,26,27). CCK-8 (Dojindo Laboratories, Inc.) was used to assess the proliferation of GC cells according to manufacturer's protocol. Briefly, AGS or HGC-27 cells were seeded into a 96-well plate at a density of ~$4x10^3$ cells/well. The absorbance was evaluated at 450 nm using a microplate reader (Tecan Group, Ltd.). For the colony formation assay, equal numbers (500 cells/well) of GC cells were seeded into 6-well plates and cultured in complete growth medium at 37˚C. After 14 days of incubation, colonies were fixed with 4% paraformaldehyde for 20 min and stained with 0.1% crystal violet solution (Sangon Biotech Co., Ltd.) for 30 min, both at room temperature. Images of the visible colonies in each well were subsequently captured, and colonies were quantified using ImageJ software (version 1.54k; National Institutes of Health).

Cell migration and invasion assays. A Transwell chamber (8 μm pore size; Corning, Inc.) precoated with Matrigel (1:8 dilution; BD Biosciences) at 37˚C for 1 h was used for invasion assays, while a Transwell chamber without Matrigel was employed for migration assays. For the AGS cells ($2x10^5$ cells/well), serum-free F12 medium was plated in the upper chamber, and F12 medium containing 20% FBS was added to the lower chamber. For the HGC-27 cells ($1x10^5$ cells/well), serum-free DMEM was used in the upper chamber, and DMEM with 20% FBS was used in the lower chamber. After 48 h of incubation at 37˚C, non-migratory cells were removed with a cotton swab, while migratory cells were fixed and stained with 0.1% crystal violet (Sangon Biotech Co., Ltd.) for 30 min at room temperature. The wells were examined under an Olympus IX70 light microscope (Olympus Corporation), and cells were counted in at least three randomly selected fields per well.

Flow cytometry. AGS and HGC-27 cells were cultured and harvested. Apoptosis was detected using the APC Annexin V Apoptosis Detection Kit with 7-AAD (cat. no. 640930; BioLegend, Inc.). Briefly, GC cells were resuspended in 1X binding buffer at a density of $1x10^6$ cells/ml and then incubated with 5 μl annexin V-APC and 5 μl 7-AAD for 15 min at 25˚C in the dark. Samples were analyzed using a FACS Canto II flow cytometer (BD Biosciences) and FlowJo v10.7.1 (BD Biosciences).

The cell cycle distribution was assessed by flow cytometry after PI staining (cat. no. C1052; Beyotime Biotechnology). Briefly, GC cells were fixed with 70% cold ethanol on ice for 60 min. The cells were washed with PBS three times and stained with PI solution in the dark for 30 min at 37˚C. Finally, the cell cycle distribution was analyzed using a FACS Canto II flow cytometer (BD Biosciences). The percentages of cells in the G_0/G_1, S and G_2/M phases were analyzed using ModFit LT 4.1 software (Verity Software House, Inc.).

Nude mouse xenograft model. The Animal Ethics Committee of the First Affiliated Hospital of Anhui Medical University granted approval for this protocol (approval no. LLSC20240221; Hefei, China). Female BALB/c nude mice (5-6 weeks old; weight, 18-22 g) were obtained from Beijing Vital River Laboratory Animal Technology Co., Ltd.

A total of 16 mice were housed under specific pathogen-free conditions in an air-conditioned room (22±2˚C) with a 12/12 h light/dark cycle and 60-65% relative humidity. The mice were provided with *ad libitum* access to food and water. First, the encoder carried out randomization using a random number table to assign mice into four groups (n=4 per group). Each mouse was marked with an ear tag for identification, and the correspondence between coded groups and experimental groups was established. Second, without knowledge of the tumor suspension assignments or mouse group identities, the experimenters established the cell-derived xenograft (CDX) model. HGC-27 cells stably transfected with either the empty vector or the EFNB2 vector were inoculated subcutaneously into the groin of the mice at a dose of $1x10^7$ cells per mouse, suspended in 100 μl PBS. DIF-3 was administered via peritumoral subcutaneous injection twice a week at a concentration of 50 μM and a dose of 100 μl per mouse. The control group received PBS at the same frequency and dose. Animal welfare was maximized, and pain and distress were minimized, while achieving scientific research objectives. The humane endpoints used were as follows: i) Body weight loss ≥20% of initial body weight; ii) tumor volume exceeding 2,000 mm^3; iii) tumor ulceration area ≥10 mm^2; iv) detection of tumor metastasis to other organs, such as the lungs; v) persistent vocalization, trembling or self-mutilation behavior; and vi) inability to access food or water autonomously, accompanied by signs of severe dehydration or malnutrition. All mice in the present study were subjected to daily health monitoring. Following the establishment of the subcutaneous tumor-bearing models, this frequency was ensured to be no less than twice daily to facilitate timely assessment of their condition. Tumor size was measured with a vernier caliper every 3-4 days, and the tumor volume was calculated using the following formula: (Length x $width^2$) x 0.5. A total of 28 days after injection, mice were humanely euthanized via CO_2 asphyxiation using a gradual-fill approach, with the gas introduced at a rate of 30-50% of the chamber volume/min. Cervical dislocation was subsequently performed to confirm death. Tumors were harvested and weighed. All data were recorded according to the pre-assigned identification numbers. The encoder and researchers jointly unblinded the study by verifying the correspondence between the codes and the actual group assignments. The harvested tumor tissues were subsequently processed for histological staining.

Statistical analysis. Statistical analyses were carried out using SPSS Statistics 22.0 (IBM Corp.), while graphical representations were generated with GraphPad Prism 7.0 (Dotmatics). Each experiment was performed in at least triplicate, with data presented as the mean ± SD. Q-Q plots and the Shapiro-Wilk test were used to assess the normality of data. For the comparison of two groups, paired or unpaired Student's t-tests were used when the continuous variable satisfied the assumptions of normal distribution and homogeneity of variance; the Mann-Whitney U test was used when the variable was non-continuous or when these assumptions (normality and/or homogeneity of variance) were violated. For comparisons among multiple groups, one-way ANOVA followed by Tukey's post hoc test was applied when the continuous variable satisfied the assumptions of normal distribution and homogeneity of variance; otherwise, the Kruskal-Wallis H test followed by Dunn's post hoc test was used. The relationship between EFNB2 expression and clinicopathological characteristics was examined using Pearson's χ^2 test. When the total sample size was ≥40 and at least one expected frequency was between 1 and 5, Yates' continuity correction was applied. Survival analysis was conducted using the Kaplan-Meier approach, with significance determined by the log-rank test. Multivariate analysis was conducted using the Cox proportional hazards model. $P<0.05$ (two-tailed) was considered to indicate a statistically significant difference.

Results

EFNB2 is highly expressed in GC tissues and is associated with clinicopathologic characteristics. An analysis of EFNB2 expression across 33 cancer types was performed using GEPIA, comparing tumor samples to corresponding normal tissues from healthy individuals. Analysis revealed that EFNB2 expression levels were increased in GC when comparing 408 GC tissues and 211 normal tissues (Fig. 1A). EFNB2 exhibited abnormal expression patterns in several solid malignancies, including colon adenocarcinoma, esophageal carcinoma and pancreatic adenocarcinoma (Fig. S1A). Furthermore, the independent GEO database analysis confirmed that EFNB2 was highly expressed in GC tissues compared with ANTs or normal gastric mucosa tissues (Fig. S1B and C). Analysis of data from GEPIA and Linkedomics databases demonstrated that the expression levels of EFNB2 increased with the progression of GC staging (Fig. 1B and C). EFNB2 expression levels were significantly increased in GC with advanced T stages (T3 or T4) compared with earlier T stages (T1) (Fig. 1D).

To further validate these observations, a TMA was constructed for IHC analysis utilizing a total of 180 samples, comprising 96 GC tissues and 84 ANTs. Analysis revealed elevated expression levels of EFNB2 in GC tissues (Fig. 1E and F). Furthermore, EFNB2 expression levels were significantly associated with tumor size, T stage, M stage and TNM stage. However, non-significant associations were identified between EFNB2 expression and other clinical parameters of patients with GC, including age, sex, HP infection, tumor location, histological grade, lymph node metastasis and HER2 status (Table I). Additionally, the high EFNB2 expression group exhibited increased levels of specific tumor markers, including CA199, CEA and CA50 (Fig. 1G-I). However, no significant differences in AFP, CA125 or CA153 levels were observed (Fig. S1D-F).

Upregulated EFNB2 expression is associated with poor prognosis of patients with GC. Subsequently, public databases were used to investigate the association between EFNB2 and the prognosis of patients with GC. Analysis of data from the Kaplan-Meier plotter demonstrated that EFNB2 expression was negatively associated with overall survival (OS; n=592) and disease-free survival (DFS; n=221) in patients with GC (Fig. 2A and B). The EFNB2-high expression group exhibited a 1.25-fold elevated risk of GC-related mortality compared with the low expression group. Accordingly, the median OS was shorter in the high-expression group (19.0 months) than in the low-expression group (24.5 months) (Fig. 2A and B). The

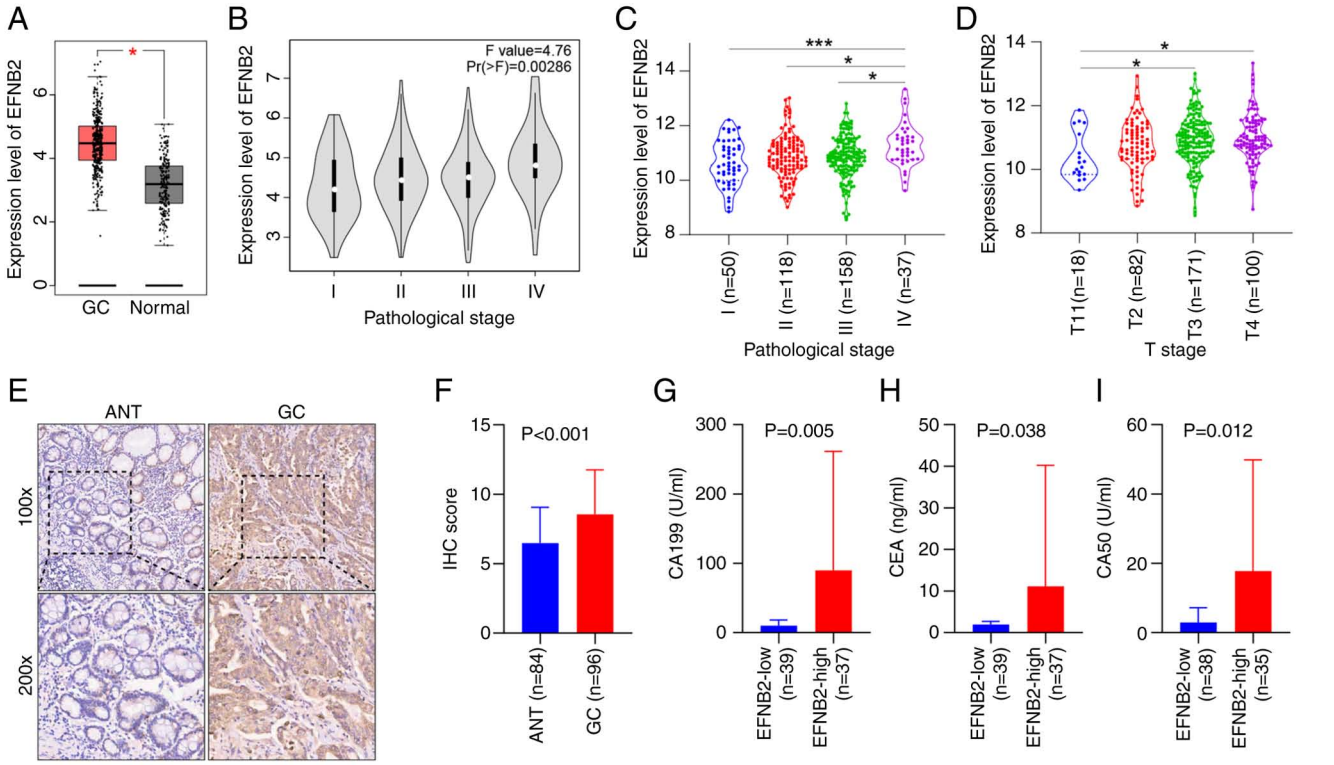

Figure 1. EFNB2 is highly expressed in GC tissues and is associated with tumor markers. (A) Expression levels of EFNB2 in GC tissues (n=408) and normal gastric mucosa tissues (n=211) in the GEPIA database (unpaired Student's t-test). (B) Analysis of data from the GEPIA database indicated the levels of EFNB2 in different pathological stages of GC (one-way ANOVA). The expression levels of EFNB2 in different (C) pathological stages and (D) T stages of GC analyzed using the Linkedomics database (one-way ANOVA). (E) Representative IHC staining images for EFNB2 in ANT and GC tissues. The magnification is indicated in the figure (x100 or x200). (F) IHC scores of EFNB2 were evaluated in 96 GC tissues and 84 ANTs (Mann-Whitney U test). The levels of different tumor markers were compared between the EFNB2-high expression group and the EFNB2-low expression group, including (G) CA199, (H) CEA and (I) CA50 (Mann-Whitney U test). *P<0.05, ***P<0.001. GC, gastric cancer; GEPIA, Gene Expression Profiling Interactive Analysis; IHC, immunohistochemical; ANT, adjacent normal tissue; EFNB2, ephrin-B2.

EFNB2-high expression group exhibited a 1.47-fold higher risk of relapse compared with the low expression group. The upper quartile DFS times were 5.3 and 3.5 months for the low and high expression groups, respectively (Fig. 2A and B). Similarly, analysis using the GEPIA database (n=383) demonstrated that high EFNB2 expression was significantly associated with worse overall prognosis and shorter time to recurrence in patients with GC (Fig. 2C and D). Notably, analysis of the GC cohort in the present study whose samples were included in the TMA (n=96) verified that high EFNB2 expression was an adverse factor for the overall prognosis of patients with GC (Fig. 2E). The median OS times of the low and high expression groups were 42 and 30 months, respectively.

The univariate analysis revealed that EFNB2 expression, tumor size, T stage, M stage and TNM stage were associated with the prognosis of patients with GC (Table II). These variables were subsequently included in a Cox proportional hazards regression model. Multivariate analysis demonstrated that only T stage remained an independent adverse prognostic factor (Table II). Furthermore, subgroup analysis of patients with GC demonstrated that high EFNB2 expression was associated with a worse prognosis in subgroups of patients with the following characteristics: Age ≥60 years, male sex, HP infection-positive, tumor location antrum, histological G2-3 grade, T stage T3-T4, lymph node metastasis-positive, M stage M0 and HER2-negative (Table III; Fig. S2).

EFNB2 promotes proliferation, inhibits apoptosis and alters the cell cycle distribution of GC cells in vitro. To explore the roles of EFNB2 in GC cells, EFNB2 levels in various GC cell lines were measured. Compared with those in human normal GES-1 cells, the expression levels of EFNB2 were higher in multiple GC cell lines (Fig. 3A and B). For the subsequent experiments, two cell lines were selected based on intrinsic EFNB2 expression levels: AGS cells (relatively high) and HGC27 cells (relatively low). EFNB2 was then knocked down in the AGS cells and overexpressed in the HGC27 cells using lentiviral transfection (40). The successful stable knockdown and overexpression of EFNB2 were verified at the protein level (Fig. 3C and D). Analysis of CCK-8 and colony formation assay data indicated that EFNB2 knockdown inhibited the proliferation and cell viability compared with those in the NC group in AGS cells. Reciprocally, EFNB2 overexpression promoted these cellular properties in HGC-27 cells (Fig. 3E-G). However, the alteration of EFNB2 levels had a non-significant effect on cell invasion and migration in GC cells (Fig. S3A-C). Additionally, analysis of data from the TIMER database indicated that the infiltration of $CD8^{+}$ T cells and neutrophils in GC tissues was negatively associated with EFNB2 expression levels, while a non-significant relationship was found with the infiltration of macrophages or dendritic cells (Fig. S3D). These data indicated that EFNB2 serves a key role in the malignant progression of GC.

Table II. Univariate and multivariate analyses for prognostic factors of gastric cancer.

	Univariate analysis		Multivariate analysis	
Parameters	HR (95% CI)	P-value	HR (95% CI)	P-value
Age (≥60 vs. <60 years)	1.453 (0.896-2.355)	0.130	-	-
Sex (male vs. female)	1.113 (0.642-1.932)	0.702	-	-
Helicobacter pylori infection (positive vs. negative)	0.713 (0.413-1.229)	0.223	-	-
Tumor location (cardia + gastric body vs. antrum)	0.927 (0.549-1.565)	0.776	-	-
Histological grade (G1 vs. G2-G3)	1.151 (0.549-2.414)	0.710	-	-
Tumor size (≥4 vs. <4 cm)	2.315 (1.411-3.797)	0.001[a]	1.368 (0.687-2.726)	0.373
T stage (T1-T2 vs. T3-T4)	3.348 (1.695-6.614)	0.001[a]	2.385 (1.112-5.113)	0.026[a]
Lymph node metastasis (positive vs. negative)	1.709 (0.971-3.008)	0.063	-	-
M stage (M0 vs. M1)	3.149 (1.687-5.880)	<0.001[a]	1.731 (0.870-3.444)	0.118
TNM stage (I-II vs. III-IV)	2.813 (1.689-4.684)	<0.001[a]	1.428 (0.741-2.751)	0.287
HER2 (positive vs. negative)	1.990 (0.851-4.651)	0.112	-	-
EFNB2 expression (high vs. low)	2.257 (1.381-3.689)	0.001[a]	1.300 (0.688-2.456)	0.419

[a]P<0.05. HR, hazard ratio; EFNB2, ephrin-B2.

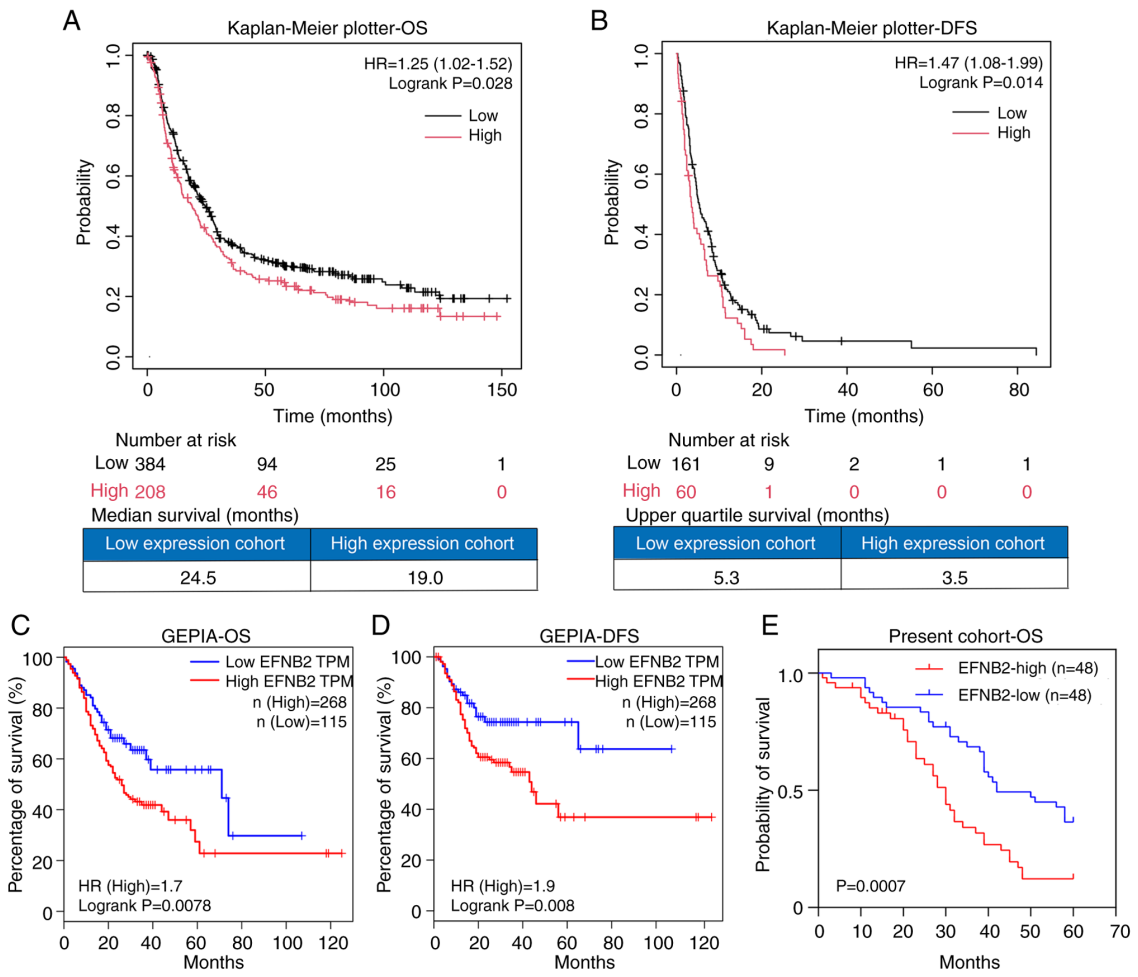

Figure 2. Upregulated EFNB2 expression is associated with poor prognosis of patients with GC. The Kaplan-Meier plotter demonstrated that EFNB2 was not only associated with (A) OS (P=0.028), but also served as a negative factor for (B) DFS in GC (P=0.014), when excluding the dataset GSE62254. In the GEPIA database, the EFNB2-high expression group exhibited shorter (C) OS and (D) DFS compared with the EFNB2-low expression group, with the conditions set as 'Cutoff-High vs. Cutoff-Low: 30 vs. 30' (P=0.0078 and 0.008, respectively). (E) Analysis of the cohort of patients whose samples were included in the tissue microarray (n=96) demonstrated that patients with GC with high EFNB2 expression had a worse clinical outcome compared with those with low EFNB2 expression (P=0.0007). OS, overall survival; DFS, disease-free survival; HR, hazard ratio; EFNB2, ephrin-B2; GC, gastric cancer; GEPIA, Gene Expression Profiling Interactive Analysis; TPM, transcript per million.

Table III. Prognostic relevance of EFNB2 expression in subgroups of patients with GC in which the worse overall survival of patients with GC is significantly associated with high EFNB2 expression.

Subgroups	HR	95% CI	P-value
Age ≥60 years	2.846	1.421-5.700	0.0032
Male	2.367	1.308-4.282	0.0044
HP infection, positive	3.028	1.312-6.986	0.0094
Tumor location, antrum	3.385	1.867-6.135	<0.0001
Histological grade, G2-G3	2.825	1.639-4.868	0.0002
T stage, T3-T4	2.166	1.261-3.719	0.0051
Lymph node metastasis, positive	2.727	1.522-4.889	0.0008
M stage, M0	2.493	1.381-4.500	0.0024
HER2, negative	2.548	1.465-4.433	0.0009

EFNB2, ephrin-B2; GC, gastric cancer; HR, hazard ratio; HP, *Helicobacter pylori*.

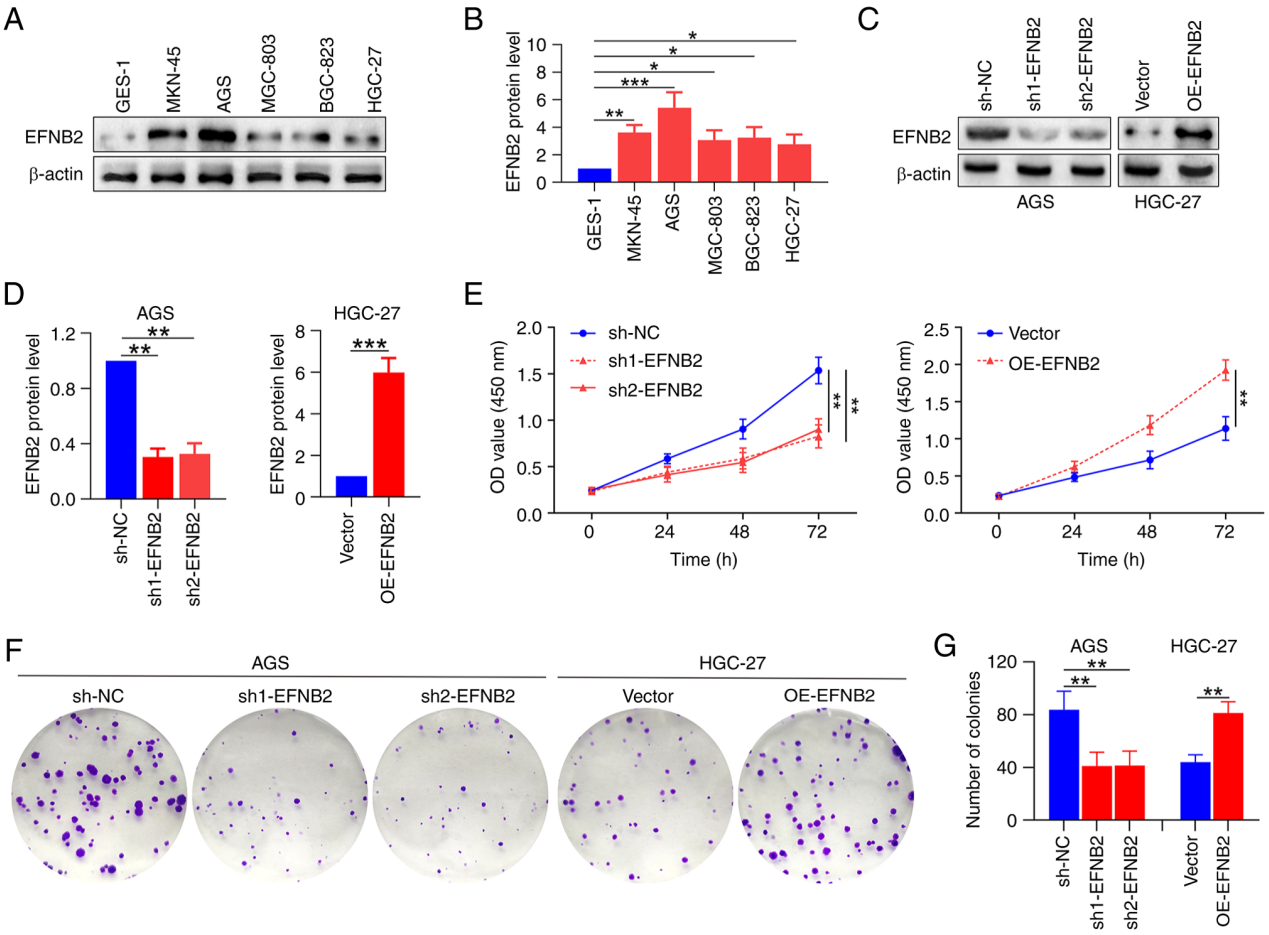

Figure 3. EFNB2 promotes the proliferation and viability of GC cells *in vitro*. (A) Representative western blot bands. (B) Expression levels of EFNB2 were detected in multiple GC cell lines and human GES-1 normal gastric mucosal epithelial cells using western blotting (one-way ANOVA). (C) Representative western blot bands. (D) The effects of EFNB2 knockdown and overexpression were verified by western blotting (one-way ANOVA for AGS cells; unpaired Student's test for HGC-27 cells). (E) Cell Counting Kit-8 assays revealed the OD values at 450 nm after 0, 24, 48 and 72 h (one-way ANOVA). (F) Representative colony formation assay images. (G) Colony formation was assessed by counting the number of colonies in various groups (one-way ANOVA for AGS cells; unpaired Student's test for HGC-27 cells). Data are presented as the mean ± SD. *P<0.05, **P<0.01, ***P<0.001. GC, gastric cancer; EFNB2, ephrin-B2; OD, optical density; OE, overexpression vector; sh, short hairpin RNA; NC, negative control.

Apoptosis and cell cycle regulation were next examined, as both are key factors influencing cell proliferation. Flow cytometry and cell cycle analysis revealed that EFNB2 knockdown elevated the proportion of apoptotic cells and quiescent period G_0/G_1 arrest, and decreased the proportions of cells in the G_2/M and S stages (Fig. 4A-D). Similarly, EFNB2

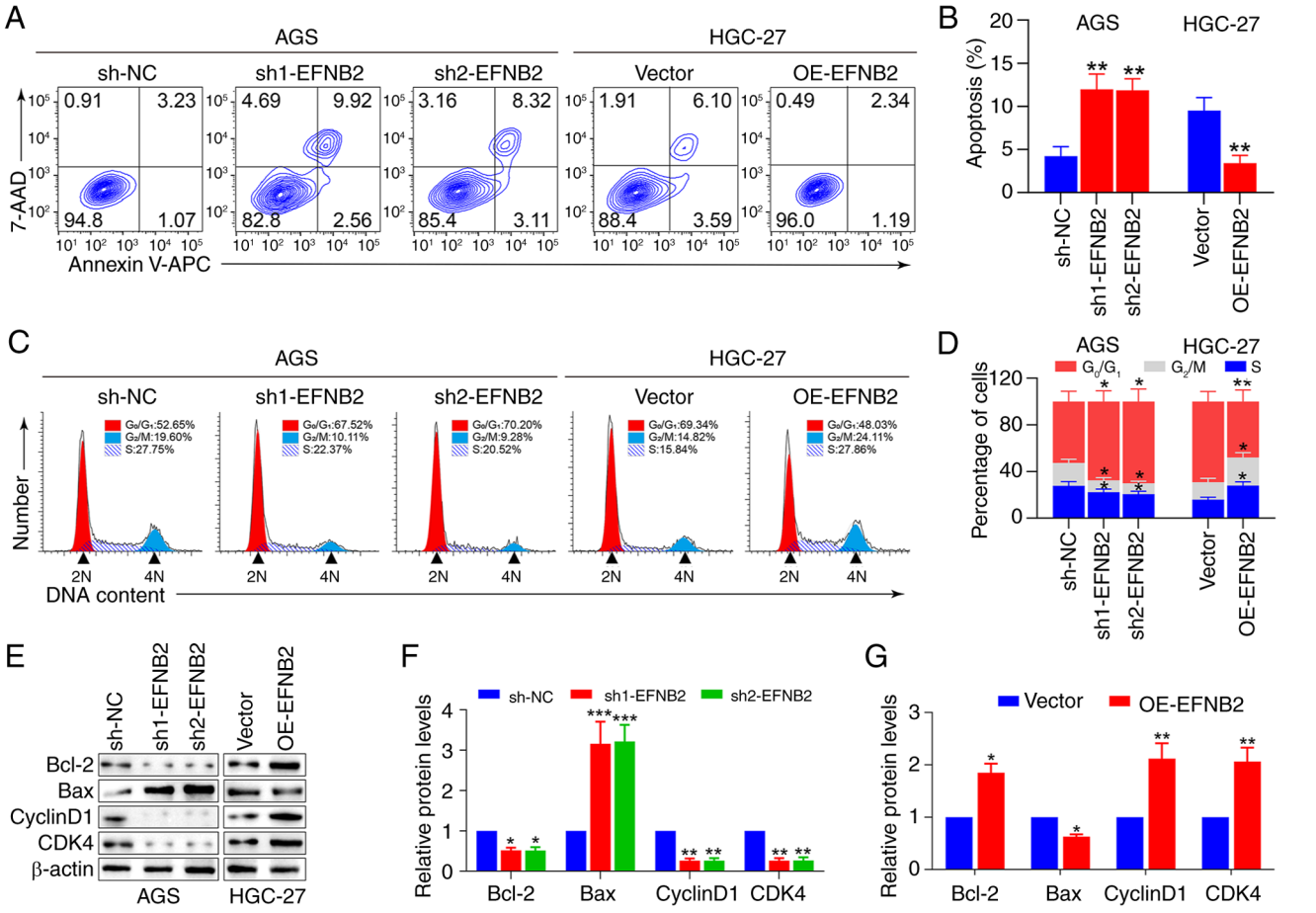

Figure 4. EFNB2 inhibits apoptosis and alters the cell cycle distribution in gastric cancer cells *in vitro*. (A) Representative flow cytometry plots and (B) quantification of apoptosis in AGS and HGC-27 cells (one-way ANOVA for AGS cells; unpaired Student's test for HGC-27 cells). (C) Representative cell cycle distribution plots and (D) quantification for the EFNB2 knockdown and overexpression groups as assessed by flow cytometry (one-way ANOVA). (E) Representative western blot bands and semi-quantification of protein expression levels of apoptosis-related proteins (Bcl-2 and Bax) and cell cycle-related proteins (CyclinD1 and CDK4) detected in the context of EFNB2 (F) knockdown or (G) overexpression (one-way ANOVA for AGS cells; unpaired Student's test for HGC-27 cells). Data are presented as the mean ± SD. *P<0.05, **P<0.01, ***P<0.001 vs. sh-NC or vector group. EFNB2, ephrin-B2; AAD, amino-actinomycin D; APC, allophycocyanin; OE, overexpression vector; sh, short hairpin RNA; NC, negative control.

overexpression reduced the proportion of apoptotic cells and quiescent period G_0/G_1 arrest, and increased the proportions of cells in the G_2/M and S stages (Fig. 4A-D). Furthermore, apoptosis-related and cell cycle-associated proteins were evaluated. Analysis revealed that the expression levels of anti-apoptosis factor Bcl-2 were decreased, whereas those of pro-apoptosis protein Bax were elevated, and the levels of CyclinD1 and CDK4 were decreased following EFNB2 knockdown (Fig. 4E-G). Correspondingly, the level of Bcl-2 was upregulated, while the level of Bax was downregulated, and the expression levels of CyclinD1 and CDK4 were elevated following EFNB2 overexpression (Fig. 4E-G). These findings indicated that EFNB2 facilitated cell proliferation by reducing apoptosis and influencing the cell cycle.

Wnt/β-catenin signaling pathway is responsible for EFNB2-mediated biological effects in GC cells. To further explore the potential mechanisms by which EFNB2 promotes cell proliferation, the correlation modules of public databases were explored. Data obtained from GEPIA and TIMER databases demonstrated significant correlations between EFNB2 expression and the levels of GSK3β, catenin β1 and its downstream effector MYC in GC (Fig. 5A and B), suggesting EFNB2 may carry out a biological role via the Wnt/β-catenin signaling pathway. The independent GSE184336 dataset (n=231) also confirmed the aforementioned associations (Fig. S3E). Emerging studies have highlighted the frequent disruption of the Wnt/β-catenin signaling pathway in GC, which is associated with aggressive tumor cell proliferation and unfavorable outcomes (19,21,41). Subsequently, the changes in Wnt/β-catenin pathway-associated proteins in response to modulated EFNB2 expression were assessed. The findings demonstrated that knockdown of EFNB2 decreased the p-GSK3β/GSK3β ratio, as well as the protein levels of β-catenin and its downstream target c-myc (Fig. 5C). Reciprocally, EFNB2 overexpression increased the p-GSK3β/GSK3β ratio and the expression of β-catenin and downstream c-myc (Fig. 5D).

Rescue experiments were conducted utilizing the Wnt/β-catenin signaling pathway agonist CHIR99021 and inhibitor DIF-3. Western blotting revealed that CHIR99021 abolished the inhibitory effect of EFNB2 knockdown on the Wnt/β-catenin pathway, whereas DIF-3 abrogated the promoting effect of EFNB2 overexpression on this pathway

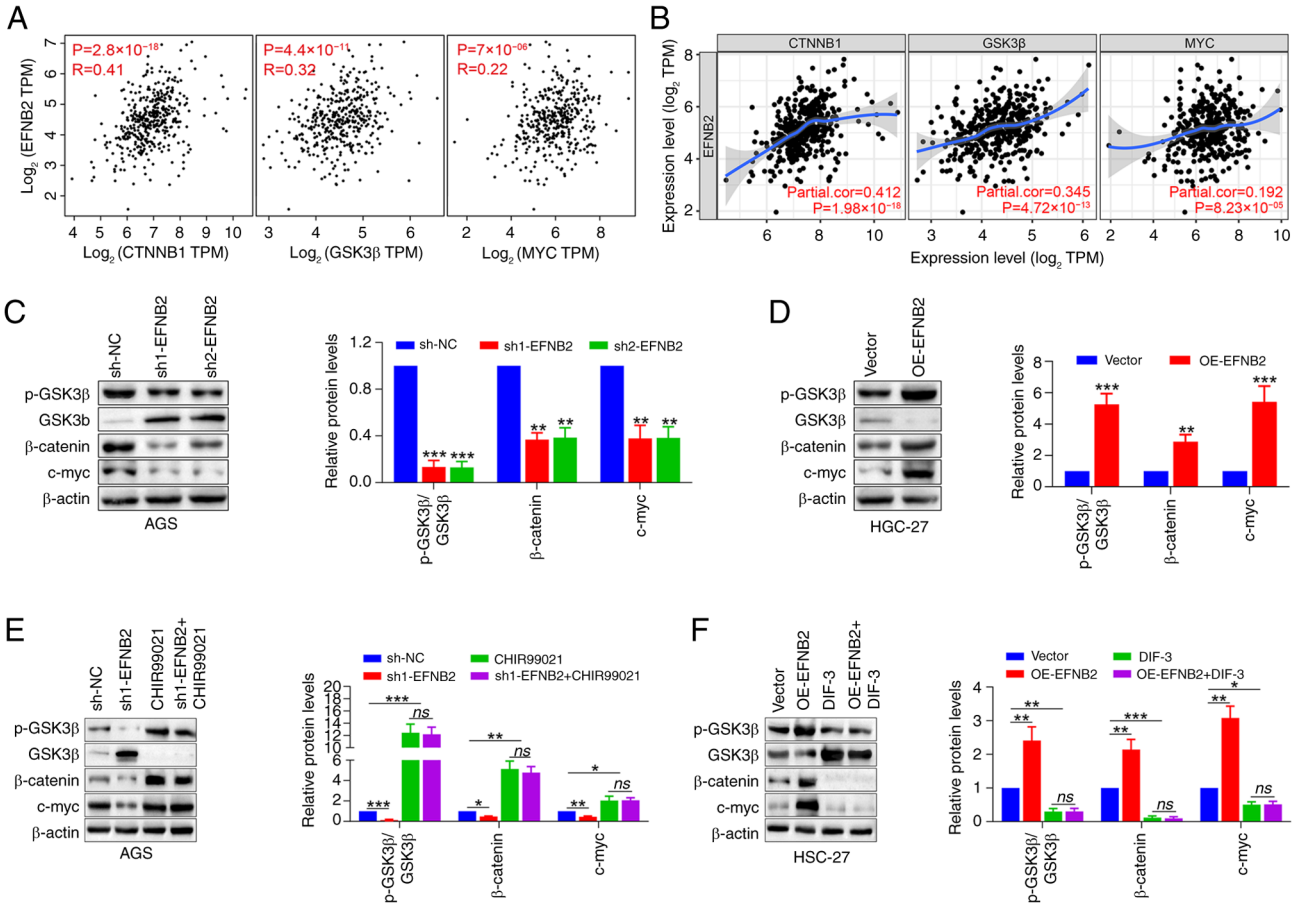

Figure 5. Wnt/β-catenin signaling pathway is responsible for EFNB2-mediated biological effects in gastric cancer cells. (A) Gene Expression Profiling Interactive Analysis and (B) Tumor Immune Estimation Resource databases were employed to explore the transcriptional correlation between EFNB2 and CTNNB1, GSK3β and downstream MYC (Spearman). Representative western blot bands and semi-quantification of protein expression levels of p-GSK3β, GSK3β, β-catenin and c-myc detected under the condition of EFNB2 (C) knockdown and (D) overexpression (one-way ANOVA for AGS cells; unpaired Student's test for HGC-27 cells). Representative western blot bands and semi-quantification of protein expression levels in the presence of (E) an agonist (CHIR99021) and (F) an inhibitor (DIF-3) of the Wnt/β-catenin signaling pathway in the EFNB2 knockdown or overexpression groups, respectively. Protein levels of p-GSK3β, GSK3β, β-catenin and c-myc were detected by western blotting (one-way ANOVA). Data are presented as the mean ± SD. *P<0.05, **P<0.01, ***P<0.001 vs. sh-NC or vector group. ns, not significant; NC, negative control; DIF-3, differentiation-inducing factor-3; p-, phosphorylated; OE, overexpression vector; sh, short hairpin RNA; CTNNB1, catenin β1; TPM, transcript per million; EFNB2, ephrin-B2.

(Fig. 5E and F). When the Wnt/β-catenin pathway was activated by CHIR99021 or inhibited by DIF-3, EFNB2 lost its regulatory effect on the pathway. Notably, DIF-3 eliminated the effects of EFNB2 on proliferation, viability, apoptosis and cell cycle regulation in GC cells (Fig. 6). These results suggested that the biological functions of EFNB2 were dependent on the activation of the Wnt/β-catenin signaling pathway.

EFNB2 promotes the tumor growth of GC through the Wnt/β-catenin signaling pathway in vivo. To further clarify whether elevated EFNB2 expression could promote tumor growth *in vivo*, a CDX mouse model was established by subcutaneously inoculating HGC-27 cell suspensions into immunodeficient nude mice and tumor growth was monitored. At 4 weeks post-injection, the xenograft tumors of the EFNB2 overexpression group had a higher volume and weight compared with those of the control group (Fig. 7A-C), suggesting that EFNB2 could effectively promote tumor growth *in vivo*. Additionally, Wnt/β-catenin pathway inhibitor DIF-3 successfully dampened GC progression and counteracted the promoting effects of EFNB2 overexpression on tumor growth *in vivo* (Fig. 7A-C). Subsequently, H&E and IHC staining were carried out (Fig. 7D). The expression levels of EFNB2 in xenograft tumors from CDX models in the EFNB2 overexpression group and the control group were assessed by IHC staining (Fig. 7D and E). The findings also demonstrated that DIF-3 abrogated the promoting effect of EFNB2 overexpression on β-catenin (Fig. 7D and E). Furthermore, Ki67 staining was used to assess the proliferative state of tumor *in vivo*. Compared with the control group, the proportion of Ki67-positive cells in EFNB2 overexpression group was increased, while DIF-3 eliminated the promoting effect of EFNB2 on proliferation in CDX models (Fig. 7D and E). TUNEL staining was used to evaluate the apoptotic condition of tumors. The proportion of apoptosis was lower in the EFNB2 overexpression group compared with the control group, while DIF-3 reversed the inhibitory effect of EFNB2 on apoptosis *in vivo* (Fig. 7D and E). These data suggested that EFNB2 accelerated the tumor growth of GC via the Wnt/β-catenin signaling pathway *in vivo*.

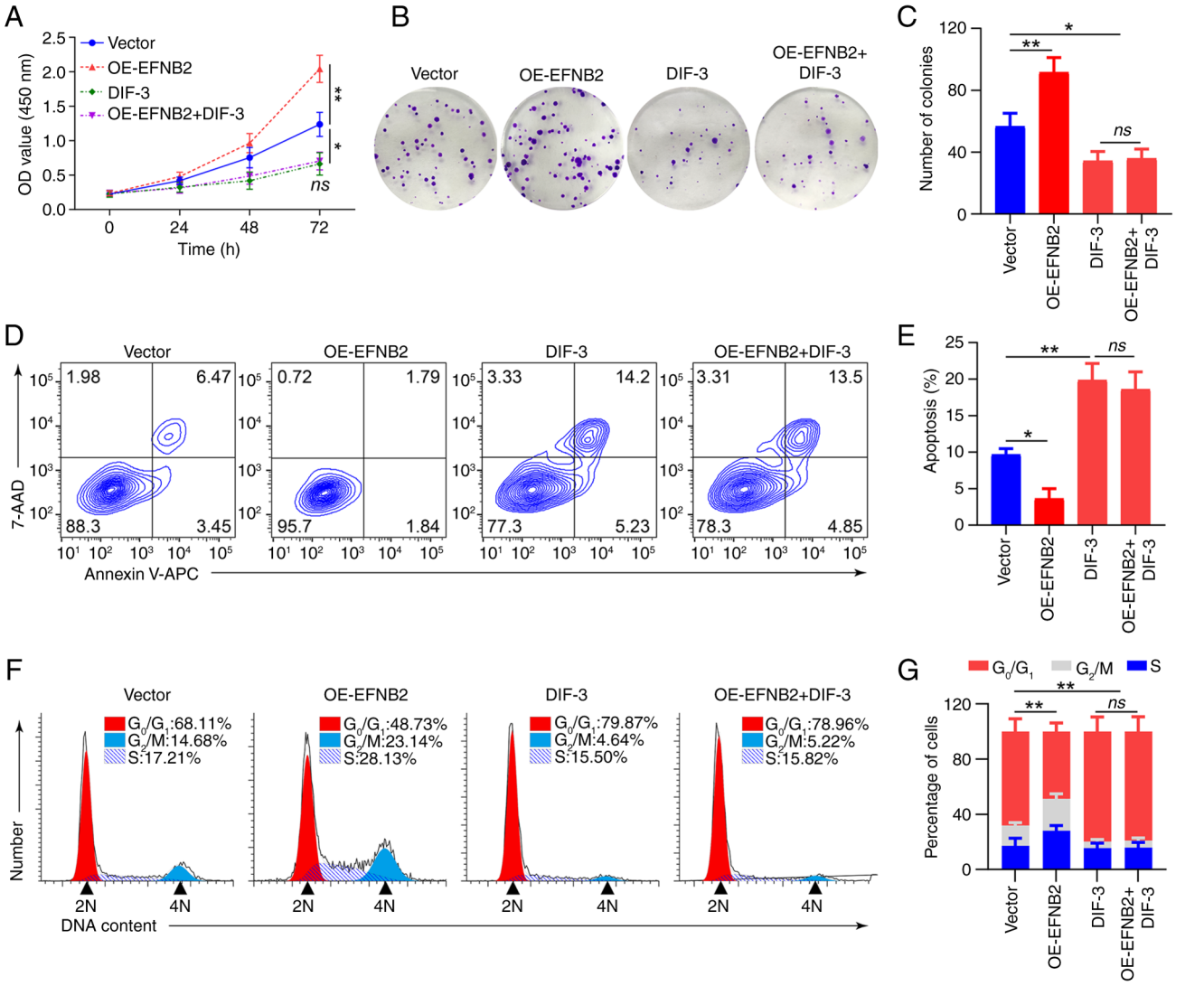

Figure 6. DIF-3 abrogates EFNB2-mediated biological effects in gastric cancer cells. (A) A Cell Counting Kit-8 was used to assess the impact of DIF-3 on HGC-27 cells transfected with EFNB2 overexpression vector in terms of proliferation (one-way ANOVA). (B) Representative images of colony formation assays. (C) Quantitative analysis of colony formation was performed to evaluate the effect of DIF-3 on EFNB2-overexpressing cells. (D and F) Representative flow cytometry plots and quantification of (E) apoptosis and (G) cell cycle distribution for the evaluation of the effect of DIF-3 on EFNB2-overexpressing cells (one-way ANOVA). Data are presented as the mean ± SD. *P<0.05, **P<0.01 vs. vector; ns, DIF-3 vs. OE-EFNB2 + DIF-3. ns, not significant; EFNB2, ephrin-B2; AAD, amino-actinomycin D; APC, allophycocyanin; DIF-3, differentiation-inducing factor-3; OD, optical density; OE, overexpression vector.

Discussion

The findings of the present study revealed a significant upregulation of EFNB2 expression in GC tissues compared with ANTs, which was inversely associated with patient prognosis, as evidenced by analysis of multiple public databases and IHC analysis of a TMA. Functional experiments indicated that EFNB2 knockdown suppressed cellular proliferation, induced apoptosis and arrested cell cycle progression *in vitro*. By contrast, overexpression of EFNB2 exhibited the opposite effect. Notably, the Wnt/β-catenin signaling pathway was identified as a key mediator of EFNB2-driven oncogenic processes in GC progression.

Accumulating clinical research supports EFNB2 as a prognostic biomarker in multiple solid tumors (42-44). In head and neck squamous cell carcinoma (HNSCC), increased EFNB2 expression has been identified as an indicator of unfavorable clinical outcomes and reduced therapeutic responsiveness (42). Similarly, in esophageal squamous cell carcinoma (ESCC), EFNB2 upregulation is inversely associated with patient survival (43). Consistent with these reports, the results of the present study demonstrated that elevated EFNB2 expression was associated with a worse prognosis in patients with GC. Notably, the consistent prognostic performance of EFNB2 across different GC subgroups underscores its potential clinical value in predicting the prognosis of patients with GC.

EFNB2 has emerged as a clinically relevant biomarker across multiple malignancies, demonstrating distinct pathological associations in various cancer types (42,43,45). In ESCC, transcriptional upregulation of EFNB2 is associated with a family history of esophageal cancer, advanced tumor stage and metastatic progression (43). In HNSCC, elevated EFNB2 mRNA levels are largely found in human papillomavirus-negative tumors arising from the oral cavity, especially in cases with alcohol intake, TP53 mutations

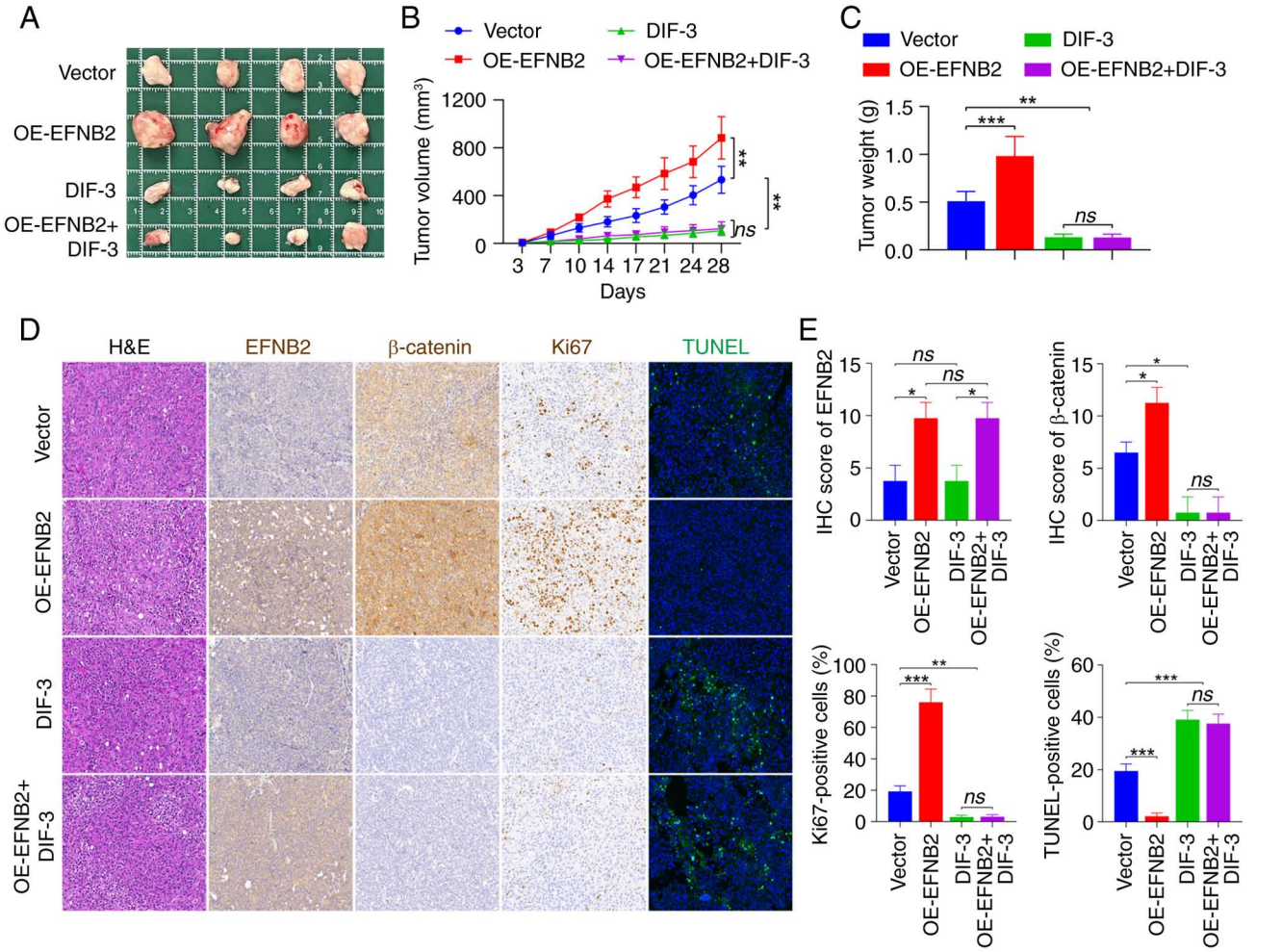

Figure 7. EFNB2 promotes the tumor growth of gastric cancer via the Wnt/β-catenin signaling pathway *in vivo*. (A) Tumors from the immunodeficient nude mice in the four experimental groups were excised and imaged. (B) Subcutaneous tumor growth (mm^3) was measured every 3-4 days following various treatments (one-way ANOVA). (C) Excised tumor masses (g) were weighed and compared across groups (one-way ANOVA). (D) Histopathological evaluation of xenograft tumors included H&E staining to examine tissue morphology, IHC analysis of EFNB2, β-catenin and Ki67 expression, and TUNEL staining for apoptotic cell evaluation. All images were captured at a magnification of x200. (E) Quantification of IHC scores for EFNB2 and β-catenin, and the percentage of positive cells for Ki67 and TUNEL staining (Kruskal-Wallis H test for EFNB2 and β-catenin; one-way ANOVA for Ki67 and TUNEL staining). Data are presented as the mean ± SD. *P<0.05, **P<0.01, ***P<0.001. ns, not significant; EFNB2, ephrin-B2; DIF-3, differentiation-inducing factor-3; OE, overexpression vector; IHC, immunohistochemical.

and EGFR amplification (42). In endometrial carcinoma, EFNB2 expression is associated with deep myometrial invasion >50% (45). The present study established a marked association between EFNB2 expression and several GC parameters, including tumor size, T/M staging, TNM classification and serum markers (CA199, CEA and CA50). However, no statistically significant association with patient demographics (age and sex), HP infection, tumor localization, histological grade, nodal involvement and HER2 expression levels was observed. Additionally, multivariate analysis demonstrated that only T stage was an independent prognostic factor, while EFNB2 expression levels did not reach statistical significance. These findings may be attributed to the excessive number of variables included in the analysis and the limited sample size, potentially leading to biased estimates in the clinicopathological and prognostic assessments. Future studies with larger sample sizes are warranted to validate these preliminary findings and obtain more reliable results.

Krusche *et al* (44) revealed that EFNB2 enhanced perivascular invasion and proliferation in glioblastoma stem-like cells by facilitating RhoA-mediated anchorage-independent cytokinesis. In colorectal cancer with mutant p53, Alam *et al* (15) reported that DNA damage-induced EFNB2 reverse signaling contributed to chemoresistance and promoted epithelial-mesenchymal transition. Conversely, EFNB2 could function as a tumor suppressor in specific types of cancer. For instance, Magic *et al* (17) found that EFNB2 suppressed cell proliferation and motility *in vitro*, and upregulated EFNB2 expression was associated with prolonged metastasis-free survival in breast cancer. Similarly, Wang *et al* (46) observed that EFNB2 decreased the migration and invasion of lung cancer cells. The role of EFNB2 varies considerably with in different tumor types, highlighting the need for further studies to fully understand its complex functions.

The results of the present study indicated that EFNB2 expression was significantly higher in GC cells and tissues, and EFNB2 could increase cell survival and proliferation

by inhibiting apoptosis and accelerating the cell cycle. EFNB2 knockdown elevated Bax levels, while reducing Bcl-2 levels, whereas EFNB2 overexpression exhibited the opposite effect. Bax and Bcl-2 are key regulators of the intrinsic apoptotic pathway (39,47), functioning by accumulating in the mitochondrial outer membrane to modulate its permeability (47). The balance between Bax-mediated pro-apoptotic signals and Bcl-2-mediated anti-apoptotic signals is important for maintaining cellular apoptosis homeostasis (40,47). Dysregulation of EFNB2 disturbed the Bcl-2/Bax equilibrium, resulting in altered apoptotic activity. EFNB2 downregulation decreased the levels of cell cycle-related proteins CDK4 and CyclinD1, while EFNB2 overexpression increased their expression. CyclinD1 and CDK4 serve a key role in the G_1-to-S-phase transition by forming a complex that drives cell cycle progression, thereby fueling cellular proliferation and tumor growth (48,49). Collectively, these alterations in protein levels point to an underlying change in the proliferative capacity of GC cells following EFNB2 dysregulation.

Previous studies have identified the Wnt/β-catenin signaling pathway as a key regulator in the progression of GC (50-52) The nuclear translocation of β-catenin activates multiple transcription factors, initiating downstream signaling networks and driving the expression of multiple proteins, including c-myc (51). Conversely, GSK3β serves a counteracting role by phosphorylating β-catenin, which accelerates its degradation and inhibits the transcriptional activity of β-catenin target genes within the nucleus (52). Additionally, the oncogenic transcription factor c-myc is dysregulated in >70% of different types of human cancer, where it drives tumorigenesis by modulating key cellular functions (53). As a transcriptional regulator, it directly controls ~15% of genomic targets, including key cell cycle components such as CyclinD1 and CDK4, thereby orchestrating cellular proliferation, differentiation and apoptosis (53). The present study demonstrated that EFNB2 knockdown decreased the phosphorylation of GSK3β, reduced β-catenin protein levels and inhibited β-catenin-mediated c-myc expression, ultimately impairing the proliferative capacity of GC cells. Conversely, EFNB2 overexpression exerted the opposite effects. EFNB2 could not only regulate p-GSK3β levels but also directly influenced the levels of total GSK3β. Although the opposite trends observed in GSK3β and p-GSK3β levels further support the conclusions, the exact molecular mechanism underlying these effects remains to be elucidated.

Rescue experiments offered additional evidence that EFNB2 regulated GC cell proliferation, apoptosis and the cell cycle via the Wnt/β-catenin signaling pathway. These *in vitro* results were further validated using CDX murine models, which substantiated the involvement of the Wnt/β-catenin pathway in EFNB2-mediated effects. Notably, although previous studies have suggested that Wnt/β-catenin signaling is involved in GC metastasis (54,55), the data in the present did not reveal a notable effect of EFNB2 expression on the migration and invasion of GC cells. This may be attributed to the involvement of other signaling pathways that counteract the effects of the Wnt/β-catenin pathway on migration and invasion. This observation further underscores the complexity of the downstream signaling networks of EFNB2, and the specific mechanisms involved require further investigation.

In summary, the expression levels of EFNB2 were higher in GC tissues compared with ANTs, and were associated with an unfavorable clinical prognosis in patients with GC. EFNB2 effectively regulated cell proliferation, apoptosis and the cell cycle in GC *in vitro*. Furthermore, EFNB2 promoted the tumor growth and malignant progression of GC *in vivo*. Mechanistically, EFNB2 exerted its oncogenic effects by activating the Wnt/β-catenin signaling pathway. Consequently, EFNB2 may be a potential molecular target for the treatment of GC.

Acknowledgements

Not applicable.

Funding

The present study was supported by the Scientific Research Fund Project of Anhui Medical University (grant no. 2023xkj225) and Key Natural Science Project of Anhui Provincial Universities (grant no. 2023AH053303).

Availability of data and materials

The data generated in the present study may be requested from the corresponding author.

Authors' contributions

DD contributed to writing the original draft, data visualization, experimental design and implementation. XW, RX, RL and YZ contributed to experimental design and implementation, data visualization, and writing, review and editing. ZW contributed to supervision, project administration, and analysis and interpretation of data. DD and ZW confirmed the authenticity of all the raw data. All authors have read and approved the final version of the manuscript.

Ethics approval and consent to participate

All animal procedures were carried out according to the protocol approved by the Animal Ethics Committee of the First Affiliated Hospital of Anhui Medical University (approval no. LLSC20240221; Hefei, China). The human tissue microarray was purchased from Shanghai Outdo Biotech Co., Ltd. (HStmA180Su32) after the approval of the Ethics Committee of the First Affiliated Hospital of Anhui Medical University (approval no. 2024137; Hefei, China).

Patient consent for publication

Not applicable.

Competing interests

The authors declare that they have no competing interests.

References

1. Bray F, Laversanne M, Sung H, Ferlay J, Siegel RL, Soerjomataram I and Jemal A: Global cancer statistics 2022: GLOBOCAN estimates of incidence and mortality worldwide for 36 cancers in 185 countries. CA Cancer J Clin 74: 229-263, 2024.
2. Chen YC, Malfertheiner P, Yu HT, Kuo CL, Chang YY, Meng FT, Wu YX, Hsiao JL, Chen MJ, Lin KP, *et al*: Global prevalence of helicobacter pylori infection and incidence of gastric cancer between 1980 and 2022. Gastroenterology 166: 605-619, 2024.
3. Onoyama T, Ishikawa S and Isomoto H: Gastric cancer and genomics: Review of literature. J Gastroenterol 57: 505-516, 2022.
4. Qiu H, Cao S and Xu R: Cancer incidence, mortality, and burden in China: A time-trend analysis and comparison with the United States and United Kingdom based on the global epidemiological data released in 2020. Cancer Commun (Lond) 41: 1037-1048, 2021.
5. Guan WL, He Y and Xu RH: Gastric cancer treatment: Recent progress and future perspectives. J Hematol Oncol 16: 57, 2023.
6. Pasquale EB: Eph receptors and ephrins in cancer: Bidirectional signalling and beyond. Nat Rev Cancer 10: 165-180, 2010.
7. Iida H, Honda M, Kawai HF, Yamashita T, Shirota Y, Wang BC, Miao H and Kaneko S: Ephrin-A1 expression contributes to the malignant characteristics of {alpha}-fetoprotein producing hepatocellular carcinoma. Gut 54: 843-851, 2005.
8. Nakada M, Drake KL, Nakada S, Niska JA and Berens ME: Ephrin-B3 ligand promotes glioma invasion through activation of Rac1. Cancer Res 66: 8492-8500, 2006.
9. Hirai H, Maru Y, Hagiwara K, Nishida J and Takaku F: A novel putative tyrosine kinase receptor encoded by the eph gene. Science 238: 1717-1720, 1987.
10. Piffko A, Uhl C, Vajkoczy P, Czabanka M and Broggini T: EphrinB2-EphB4 signaling in neurooncological disease. Int J Mol Sci 23: 1679, 2022.
11. Rutkowski R, Mertens-Walker I, Lisle JE, Herington AC and Stephenson SA: Evidence for a dual function of EphB4 as tumor promoter and suppressor regulated by the absence or presence of the ephrin-B2 ligand. Int J Cancer 131: E614-E624, 2012.
12. Piffko A, Broggini T, Harms C, Adams RH, Vajkoczy P and Czabanka M: Ligand-dependent and ligand-independent effects of Ephrin-B2-EphB4 signaling in melanoma metastatic spine disease. Int J Mol Sci 22: 8028, 2021.
13. Dai B, Shi X, Ma N, Ma W, Zhang Y, Yang T, Zhang J and He L: HMQ-T-B10 induces human liver cell apoptosis by competitively targeting EphrinB2 and regulating its pathway. J Cell Mol Med 22: 5231-5243, 2018.
14. Zhong S, Pei D, Shi L, Cui Y and Hong Z: Ephrin-B2 inhibits $A\beta_{25-35}$-induced apoptosis by alleviating endoplasmic reticulum stress and promoting autophagy in HT22 cells. Neurosci Lett 704: 50-56, 2019.
15. Alam SK, Yadav VK, Bajaj S, Datta A, Dutta SK, Bhattacharyya M, Bhattacharya S, Debnath S, Roy S, Boardman LA, *et al*: DNA damage-induced ephrin-B2 reverse signaling promotes chemoresistance and drives EMT in colorectal carcinoma harboring mutant p53. Cell Death Differ 23: 707-722, 2016.
16. Zhu F, Dai SN, Xu DL, Hou CQ, Liu TT, Chen QY, Wu JL and Miao Y: EFNB2 facilitates cell proliferation, migration, and invasion in pancreatic ductal adenocarcinoma via the p53/p21 pathway and EMT. Biomed Pharmacother 125: 109972, 2020.
17. Magic Z, Sandström J and Perez-Tenorio G: Ephrin-B2 inhibits cell proliferation and motility in vitro and predicts longer metastasis-free survival in breast cancer. Int J Oncol 55: 1275-1286, 2019.
18. Zhang Y, Zhang R, Ding X and Ai K: EFNB2 acts as the target of miR-557 to facilitate cell proliferation, migration and invasion in pancreatic ductal adenocarcinoma by bioinformatics analysis and verification. Am J Transl Res 10: 3514-3528, 2018.
19. Akhavanfar R, Shafagh SG, Mohammadpour B, Farahmand Y, Lotfalizadeh MH, Kookli K, Adili A, Siri G and Eshagh Hosseini SM: A comprehensive insight into the correlation between ncRNAs and the Wnt/β-catenin signalling pathway in gastric cancer pathogenesis. Cell Commun Signal 21: 166, 2023.
20. Clevers H: Wnt/beta-catenin signaling in development and disease. Cell 127: 469-480, 2006.
21. Mirabelli CK, Nusse R, Tuveson DA and Williams BO: Perspectives on the role of Wnt biology in cancer. Sci Signal 12: eaay4494, 2019.
22. Lien WH and Fuchs E: Wnt some lose some: Transcriptional governance of stem cells by Wnt/β-catenin signaling. Genes Dev 28: 1517-1532, 2014.
23. Tang Z, Li C, Kang B, Gao G, Li C and Zhang Z: GEPIA: A web server for cancer and normal gene expression profiling and interactive analyses. Nucleic Acids Res 45: W98-W102, 2017.
24. Vasaikar SV, Straub P, Wang J and Zhang B: LinkedOmics: Analyzing multi-omics data within and across 32 cancer types. Nucleic Acids Res 46: D956-D963, 2018.
25. Győrffy B: Survival analysis across the entire transcriptome identifies biomarkers with the highest prognostic power in breast cancer. Comput Struct Biotechnol J 19: 4101-4109, 2021.
26. Li T, Fan J, Wang B, Traugh N, Chen Q, Liu JS, Li B and Liu XS: TIMER: A web server for comprehensive analysis of tumor-infiltrating immune cells. Cancer Res 77: e108-e110, 2017.
27. Cristescu R, Lee J, Nebozhyn M, Kim KM, Ting JC, Wong SS, Liu J, Yue YG, Wang J, Yu K, *et al*: Molecular analysis of gastric cancer identifies subtypes associated with distinct clinical outcomes. Nat Med 21: 449-456, 2015.
28. Kim HK, Choi IJ, Kim CG, Kim HS, Oshima A, Michalowski A and Green JE: A gene expression signature of acquired chemoresistance to cisplatin and fluorouracil combination chemotherapy in gastric cancer patients. PLoS One 6: e16694, 2011.
29. Ooi CH, Ivanova T, Wu J, Lee M, Tan IB, Tao J, Ward L, Koo JH, Gopalakrishnan V, Zhu Y, *et al*: Oncogenic pathway combinations predict clinical prognosis in gastric cancer. PLoS Genet 5: e1000676, 2009.
30. Förster S, Gretschel S, Jöns T, Yashiro M and Kemmner W: THBS4, a novel stromal molecule of diffuse-type gastric adenocarcinomas, identified by transcriptome-wide expression profiling. Mod Pathol 24: 1390-1403, 2011.
31. Wang G, Hu N, Yang HH, Wang L, Su H, Wang C, Clifford R, Dawsey EM, Li JM, Ding T, *et al*: Comparison of global gene expression of gastric cardia and noncardia cancers from a high-risk population in china. PLoS One 8: e63826, 2013.
32. Busuttil RA, George J, Tothill RW, Ioculano K, Kowalczyk A, Mitchell C, Lade S, Tan P, Haviv I and Boussioutas A: A signature predicting poor prognosis in gastric and ovarian cancer represents a coordinated macrophage and stromal response. Clin Cancer Res 20: 2761-2772, 2014.
33. Cheng L, Yang S, Yang Y, Zhang W, Xiao H, Gao H, Deng X and Zhang Q: Global gene expression and functional network analysis of gastric cancer identify extended pathway maps and GPRC5A as a potential biomarker. Cancer Lett 326: 105-113, 2012.
34. Lou S, Zhang J, Yin X, Zhang Y, Fang T, Wang Y and Xue Y: Comprehensive characterization of tumor purity and its clinical implications in gastric cancer. Front Cell Dev Biol 9: 782529, 2022.
35. Fang C, Wang W, Deng JY, Sun Z, Seeruttun SR, Wang ZN, Xu HM, Liang H and Zhou ZW: Proposal and validation of a modified staging system to improve the prognosis predictive performance of the 8th AJCC/UICC pTNM staging system for gastric adenocarcinoma: A multicenter study with external validation. Cancer Commun (Lond) 38: 67, 2018.
36. Liu Q, Li Y, Niu Z, Zong Y, Wang M, Yao L, Lu Z, Liao Q and Zhao Y: Atorvastatin (Lipitor) attenuates the effects of aspirin on pancreatic cancerogenesis and the chemotherapeutic efficacy of gemcitabine on pancreatic cancer by promoting M2 polarized tumor associated macrophages. J Exp Clin Cancer Res 35: 33, 2016.
37. Shen J, Cao B, Wang Y, Ma C, Zeng Z, Liu L, Li X, Tao D, Gong J and Xie D: Hippo component YAP promotes focal adhesion and tumour aggressiveness via transcriptionally activating THBS1/FAK signalling in breast cancer. J Exp Clin Cancer Res 37: 175, 2018.
38. Zhang Y, Liu Q, Liu J and Liao Q: Upregulated CD58 is associated with clinicopathological characteristics and poor prognosis of patients with pancreatic ductal adenocarcinoma. Cancer Cell Int 21: 327, 2021.
39. Zhang Y, Liu Q, Yang S and Liao Q: Knockdown of LRRN1 inhibits malignant phenotypes through the regulation of HIF-1α/notch pathway in pancreatic ductal adenocarcinoma. Mol Ther Oncolytics 23: 51-64, 2021.
40. Zhang Y, Zhang R, Luo G and Ai K: Long noncoding RNA SNHG1 promotes cell proliferation through PI3K/AKT signaling pathway in pancreatic ductal adenocarcinoma. J Cancer 9: 2713-2722, 2018.

41. Han R, Yang J, Zhu Y and Gan R: Wnt signaling in gastric cancer: Current progress and future prospects. Front Oncol 14: 1410513, 2024.
42. Oweida A, Bhatia S, Hirsch K, Calame D, Griego A, Keysar S, Pitts T, Sharma J, Eckhardt G, Jimeno A, *et al*: Ephrin-B2 overexpression predicts for poor prognosis and response to therapy in solid tumors. Mol Carcinog 56: 1189-1196, 2017.
43. Ni Q, Chen P, Zhu B, Li J, Xie D and Ma X: Expression levels of *EPHB4*, *EFNB2* and caspase-8 are associated with clinicopathological features and progression of esophageal squamous cell cancer. Oncol Lett 19: 917-929, 2020.
44. Krusche B, Ottone C, Clements MP, Johnstone ER, Goetsch K, Lieven H, Mota SG, Singh P, Khadayate S, Ashraf A, *et al*: EphrinB2 drives perivascular invasion and proliferation of glioblastoma stem-like cells. Elife 5: e14845, 2016.
45. Takai N, Miyazaki T, Fujisawa K, Nasu K and Miyakawa I: Expression of receptor tyrosine kinase EphB4 and its ligand ephrin-B2 is associated with malignant potential in endometrial cancer. Oncol Rep 8: 567-573, 2001.
46. Wang L, Peng Q, Sai B, Zheng L, Xu J, Yin N, Feng X and Xiang J: Ligand-independent EphB1 signaling mediates TGF-β-activated CDH2 and promotes lung cancer cell invasion and migration. J Cancer 11: 4123-4131, 2020.
47. Peña-Blanco A and García-Sáez AJ: Bax, Bak and beyond-mitochondrial performance in apoptosis. FEBS J 285: 416-431, 2018.
48. Tchakarska G and Sola B: The double dealing of cyclin D1. Cell Cycle 19: 163-178, 2020.
49. Ziegler DV, Parashar K and Fajas L: Beyond cell cycle regulation: The pleiotropic function of CDK4 in cancer. Semin Cancer Biol 98: 51-63, 2024.
50. Koushyar S, Powell AG, Vincan E and Phesse TJ: Targeting Wnt signaling for the treatment of gastric cancer. Int J Mol Sci 21: 3927, 2020.
51. Liu J, Xiao Q, Xiao J, Niu C, Li Y, Zhang X, Zhou Z, Shu G and Yin G: Wnt/β-catenin signalling: Function, biological mechanisms, and therapeutic opportunities. Signal Transduct Target Ther 7: 3, 2022.
52. Zhang Y and Wang X: Targeting the Wnt/β-catenin signaling pathway in cancer. J Hematol Oncol 13: 165, 2020.
53. Madden SK, de Araujo AD, Gerhardt M, Fairlie DP and Mason JM: Taking the Myc out of cancer: Toward therapeutic strategies to directly inhibit c-Myc. Mol Cancer 20: 3, 2021.
54. Xue W, Yang L, Chen C, Ashrafizadeh M, Tian Y and Sun R: Wnt/β-catenin-driven EMT regulation in human cancers. Cell Mol Life Sci 81: 79, 2024.
55. Wu C, Zhuang Y, Jiang S, Liu S, Zhou J, Wu J, Teng Y, Xia B, Wang R and Zou X: Interaction between Wnt/β-catenin pathway and microRNAs regulates epithelial-mesenchymal transition in gastric cancer (review). Int J Oncol 48: 2236-2246, 2016.